frontiers in Physics

ORIGINAL RESEARCH
published: 28 October 2020
doi: 10.3389/fphy.2020.589334

Construction of a Cost-Effective Phased Array Through High-Efficiency Transmissive Programable Metasurface

Anjie Cao[1,2]*, *Zhansheng Chen*[1], *Kai Fan*[1], *Yuehui You*[1] and *Chong He*[2]

[1] R&D center, Shanghai Institute of Satellite Engineering, Shanghai, China, [2] Department of Electronic Engineering, Shanghai Jiao Tong University, Shanghai, China

Programmable metasurfaces have shown great potential in the areas of low-complexity phase array systems in comparison with the conventional phased array antennas. In this document, a 1-bit transmissive programable metasurface with high efficiency is proposed for the cost-effective beam-steering phased array. The designed transmissive metasurface is made up of reconfigurable cells with perfect 1-bit phase tuning and less transmission losses. Through dynamically programming the 1-bit code distributions of the metasurface, real-time scanning pencil beams in desired directions can be created.

Keywords: metasurface, programmable, phased array, cost-effective, transmissive

OPEN ACCESS

Edited by:
Fajun Xiao, Northwestern Polytechnical University, China

Reviewed by:
Ke Chen, Huazhong University of Science and Technology, China
Zhongyue Zhang, Shaanxi Normal University, China
Changhong Zhang, Chongqing University of Posts and Telecommunications, China

***Correspondence:**
Anjie Cao
13774224487@163.com

Specialty section:
This article was submitted to Optics and Photonics, a section of the journal Frontiers in Physics

Received: *30 July 2020*
Accepted: *24 September 2020*
Published: *28 October 2020*

Citation:
Cao A, Chen Z, Fan K, You Y and He C (2020) Construction of a Cost-Effective Phased Array Through High-Efficiency Transmissive Programable Metasurface. Front. Phys. 8:589334. doi: 10.3389/fphy.2020.589334

INTRODUCTION

Recently, metasurfaces are widely known as a kind of two-dimensional periodic structures with subwavelength scale, owing to its independent talent of delicate modulation on electromagnetic waves [1]. Based on the advantages of low loss, easy integration and simple preparation, metasurfaces have shown extensive application prospects and become a research hotspot in modern physics, information science and the related interdisciplinary [2–4].

Within microwave domain, metasurfaces also arouse a wide range of investigation, such as radiation improvement [5–7], perfect absorbers [8, 9], OAM-EM wave generation [10–13], scattering reduction [14–16], holographic imaging [17, 18], and energy harvesting [19]. Metasurfaces particularly demonstrate the unique abilities in waveform shaping through the phase manipulation of the building units in microwave metasurfaces. Reflective metasurfaces were demonstrated to generate the high-intensity pencil beams or high-purity vortex waves through the full 2π phase tuning [20, 21]. Polarization-insensitive transmissive metasurface with hexagonal unit configuration is proposed to stimulate vortex beam at any polarization [22]. The ultra-thin transmissive metasurfaces were designed for high-efficiency wavefront modulation in circular polarization, based on photon spin Hall effect or Pancharatnam-Berry phase theory [23, 24]. Nevertheless, for all the foregoing designs, only the fixed directional or shaped beams can be created once the metasurfaces are constructed, which restrict the application for dynamic control in electromagnetic wave.

The programmable metasurfaces integrated with lumped components could be very practical for the fine-grained modulation over electromagnetic waves, which also show great advantages at improving the incomplexity and cost for dynamic beam forming or scanning, in comparison with conventional phased array systems that are composed of massive digital or analog phase shifters [25]. Digital or programmable metamaterials are firstly proposed in 2014 to expand the concept of metamaterials by using dynamic sequences of "0" and "1" bits [26]. Ulteriorly, the metasurface unit

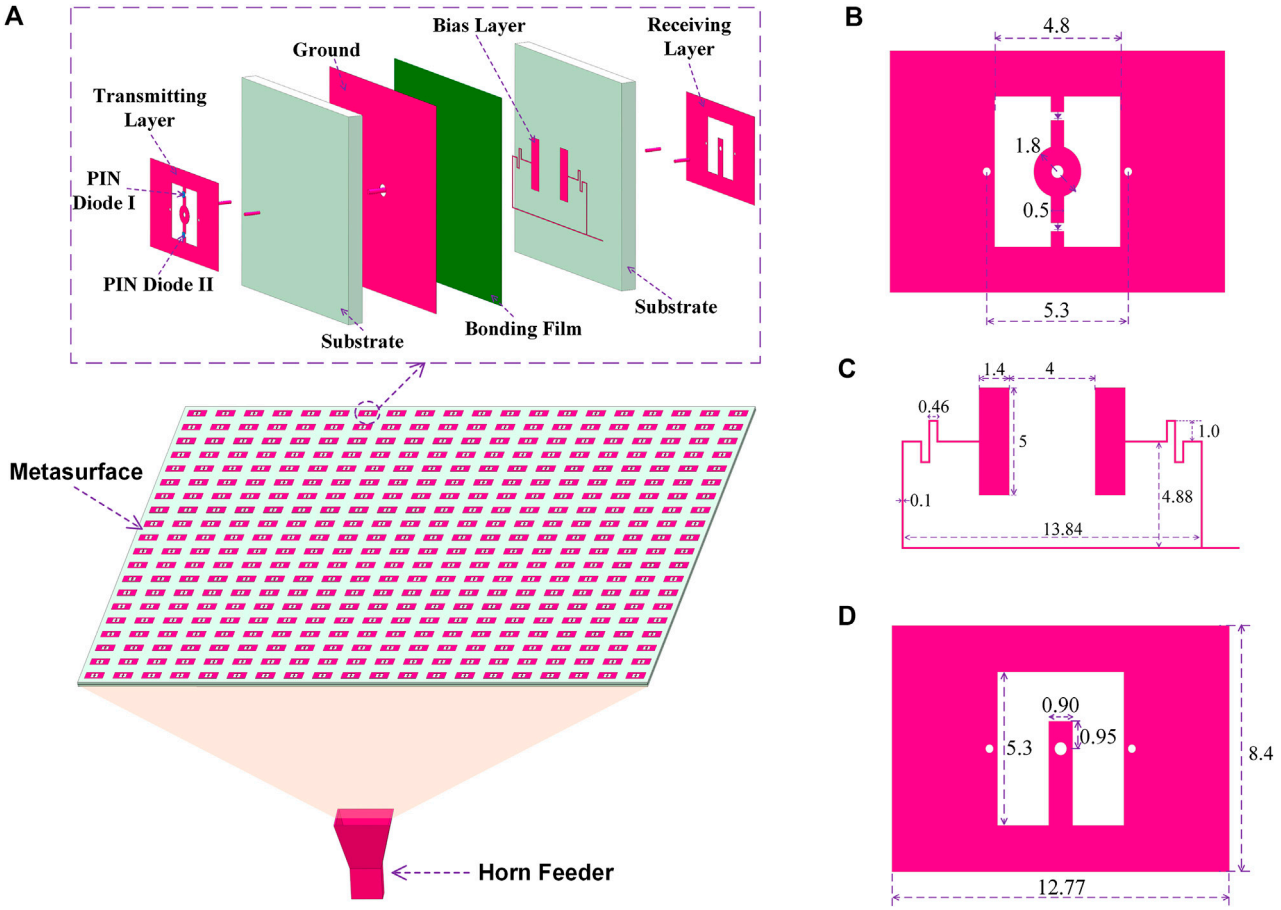

FIGURE 1 | Topological configuration of the proposed transmissive metasurface (all dimensions are in millimeters) **(A)** Exploded view of the 1-bit cell on top along with the metasurface at bottom **(B)** Transmitting layer **(C)** Bias layer **(D)** Receiving layer.

can obtain a clear alteration in resonant property through integrating lumped components, and the programmable reflective metasurfaces are thus actually constructed for the dynamic modulation of the electromagnetic waves [27]. The digital reflective metasurfaces were constructed by designing reconfigurable cells combined with the PIN diodes for binary phase states [28, 29]. Later, two-bit reflective programable metasurfaces were designed by integrating two PIN diodes or a voltage-controlled varactor diode to modulate the resonant characteristics of the reconfigurable units [30, 31]. Since the feed shielding effects and the phase distortions are usually very serious for the reflective metasurfaces, the programmable transmissive metasurfaces are then proposed to avoid these deficiencies [32]. Metasurface unit integrated with C-shaped patch and U-shaped slot serving as the receiver and transmitter was designed to construct the digital transmissive metasurface [33]. Metasurface unit with the combination of a couple of C-shaped patches and ring slots was adopted to achieve 1-bit phase resolution [34]. Later, the equivalent magnetic dipole unit was also presented by combining the rectangular patch and side-shorted patch [35]. However, all these transmissive metasurfaces are suffering from very high transmission losses due to the insufficient unit architecture design, which lead to the low aperture efficiency not exceeding 20.0%.

In this document, a high-efficiency transmissive 1-bit digital metasurface is designed for the construction of the cost-effective phased array. Through dynamically programming the 1-bit code distributions of the metasurface when biasing the integrated PIN diodes, real-time scanning pencil beams in the desired directions can be created and the numerical simulation results demonstrate the availability of the proposed metasurface.

UNIT DESIGN AND CONFIGURATION

The component of the designed transmissive programable metasurface is a reconfigurable programmable cell with binary phase modulation. The 1-bit unit is constructed with multilayer metallic structure along with two dielectric substrates and a bonding film, the structure of which is shown in **Figure 1A**. The two dielectric substrates have the same parameters with the dielectric constant of 3.55 and the thickness of 1.524 mm, and the thickness of the bonding film is 0.1 mm. The metallic structure is composed of the transmitting patch, the ground plane, the bias

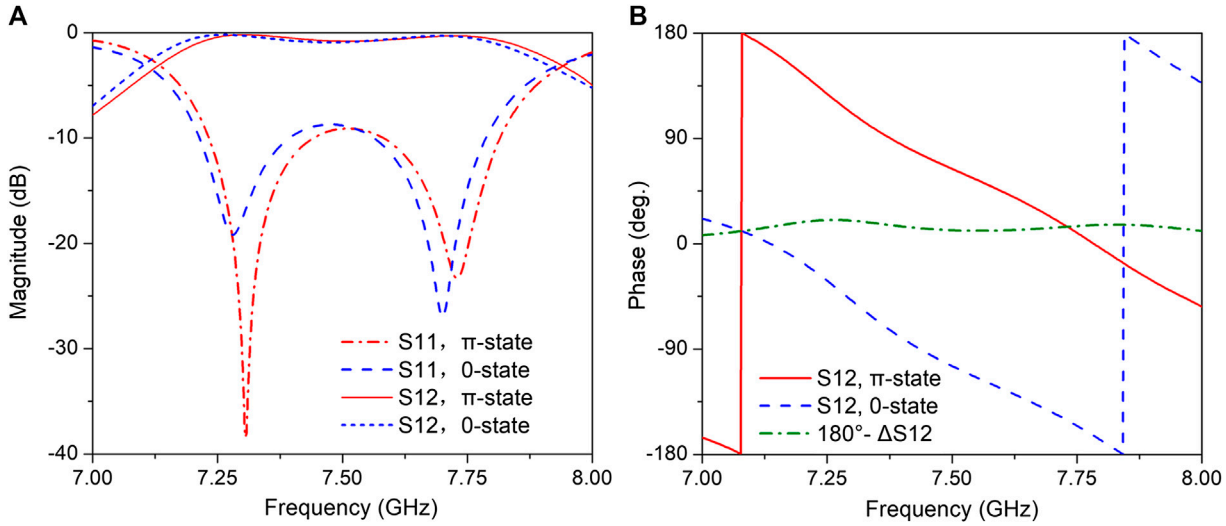

FIGURE 2 | Simulated scattering parameters of the proposed metasurface cell **(A)** Magnitude for both π/0-states **(B)** Phases for both π/0 states.

layer and the receiving patch. The transmitting patch is designed in front with a rectangular patch loaded by an O-slot and two PIN diodes, while the same-sized receiving patch is set on the reverse side and integrated by an U-slot, and the two patches constitute an integral whole by a metallized central via-hole through the ground. In addition, the transmitting patch is connected with the ground through a pair of symmetric via-holes, while the receiving patch is connected with a pair of rectangular distributed capacitors in the bias layer in similar way for biasing purpose. To reduce the influence of the bias lines on the designed unit, the bias lines are designed using extremely narrow linewidths and located near the ground plane. Detailed structure and dimensions of the proposed metasurface cell are also given in **Figure 1**.

The PIN diode M/A-COM Flip Chip MA4FCP305 is chosen to construct and modulate the unit, and the parameter modelling of the PIN diode is characterized as lumped components for the binary ON/OFF states [36]. When biasing the PIN diode with a forward current, the ON state along with a series of a resistance $R_{ON} = 2.1\ \Omega$ would be employed; and for a reverse bias voltage, the OFF state along with a parallel of a capacitance $C_{OFF} = 0.05$ pF would be applied for the PIN diode. The 1-bit phase modulation of the unit can be accomplished through biasing the integrated PIN diodes. The simulated scattering parameters of the designed metasurface cell are plotted in magnitude and phase for both π/0 states, as shown in **Figure 2**. When PIN diode I is at the ON state and PIN diode II is at the OFF state, the metasurface cell would be operating at the π-state; the simulated S_{11} is less than –10 dB from 7.23 to 7.82 GHz, and the simulated S_{12} is above –2 dB from 7.17 to 7.89 GHz. When PIN diode I is at the OFF state and PIN diode II is at the ON state, the metasurface cell would be working at the 0-state; now the simulated S_{11} is less than –10 dB from 7.21 to 7.79 GHz, and the simulated S_{12} is above –2 dB from 7.13 to 7.86 GHz. The phase displacement of the binary cell states could maintain constant at nearby π with relatively small variations.

METASURFACE CONFIGURATION AND BEAM-SCANNING VERIFICATION

In the actual metasurface design, the transmissive programable metasurface is constructed with 400 units and an overall dimension of 400 × 400 mm^2, and the overall structure of the designed metasurface is also shown in **Figure 1A**. The focal source of a standard waveguide horn is placed in front of the

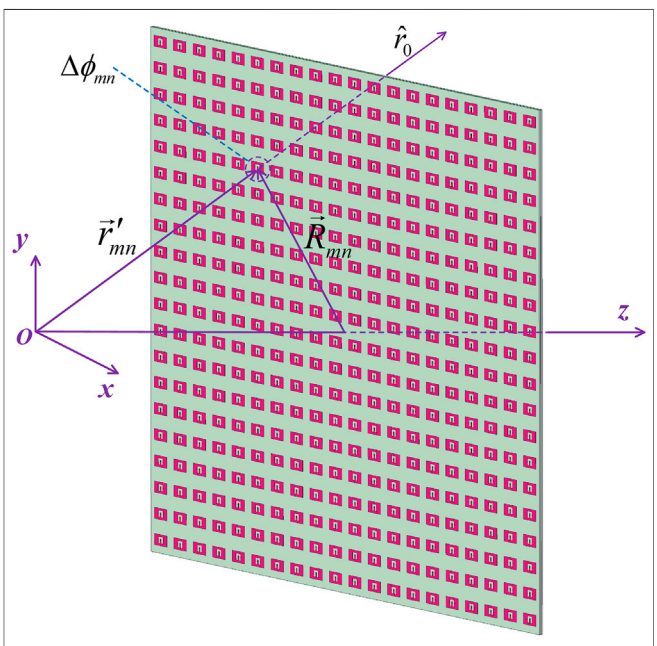

FIGURE 3 | Spatially-fed geometry and the relevant vector coordinates.

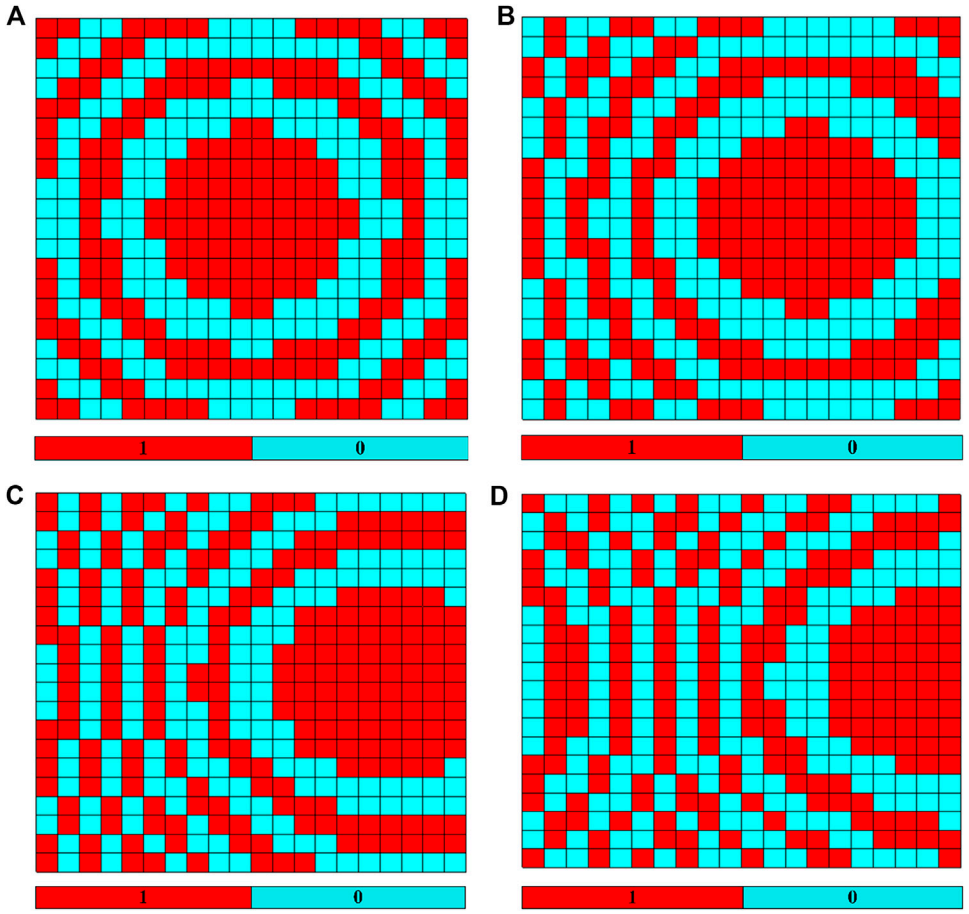

FIGURE 4 | Optimal quantized phase code distributions for four beam directions **(A)** $\theta = 0^{\circ}$ **(B)** $\theta = 15^{\circ}$ **(C)** $\theta = 30^{\circ}$ **(D)** $\theta = 45^{\circ}$.

central axis of the metasurface with a focal length of F = 5λ = 200 mm, and the cells on the metasurface serve as the 1-bit phase shifters for the incoming wave and are modulated through the bias layer.

To generate a scanning pencil beam in the desired direction, the phase compensation $\Delta\phi_{mn}$ for the metasurface cells should satisfy the formula,

$$k_0\left(r'_{mn} - \overrightarrow{R}_{mn} \cdot \hat{r}_0\right) - \Delta\phi_{mn} = 2n\pi \quad n \in Z \tag{1}$$

where k_0 is the wavenumber, $\overrightarrow{r}'_{mn}$ is the position vector of the mnth unit, $\overrightarrow{R}_{mn}$ is the position vector of the mnth unit relative to $(0, 0, f)$, and $\hat{r}_0$ is the desired direction of the pencil beam. All these parameters are defined as shown in **Figure 3**.

To get the overall code distribution on the metasurface, the binary phase states for each unit could be obtained by furtherly quantizing the continuous phase shift $\Delta\phi_{mn}$,

$$\phi_Q = \begin{cases} 0, & \Delta\phi_{mn} \in [0 + 2n\pi, \pi + 2n\pi) \\ \pi, & \Delta\phi_{mn} \in [\pi + 2n\pi, 2\pi + 2n\pi) \end{cases} \quad n \in Z \tag{2}$$

To furtherly validate the effectiveness of the transmissive programmable metasurface, steering pencil beams with a wide scanning range of at least 45° and an angular spacing of 15° are then numerically generated. The optimal quantized code distributions for the four directional beams are generated using **Equation (2)** and implemented as shown in **Figure 4**, which can be simply controlled by the modulation of the ON/OFF states of the PIN diodes. The simulated far-field radiation patterns for the scanning pencil beams in four directions are plotted in **Figure 5**. For the broadside radiation, a directional beam is obtained with a simulated gain over 25.3 dB, corresponding to an aperture efficiency over 27% by using the following definition:

$$\eta = \frac{G}{4\pi A / \lambda^2} \tag{3}$$

where G is the simulated gain and A is the metasurface aperture area. When furtherly considering the quantization loss of about 3 dB for a typical 1-bit phase resolution, the metasurface aperture efficiency could be expected to exceed 50% theoretically. As the scanning angle of the steering beam increases, the main-lobe maximum gain would decrease due to the diminution of the effective metasurface aperture area, which is in accordance with the traditional phased array antenna. For all the four directional scanning beams, the side-lobe levels are −10 dB lower than that of the main lobes.

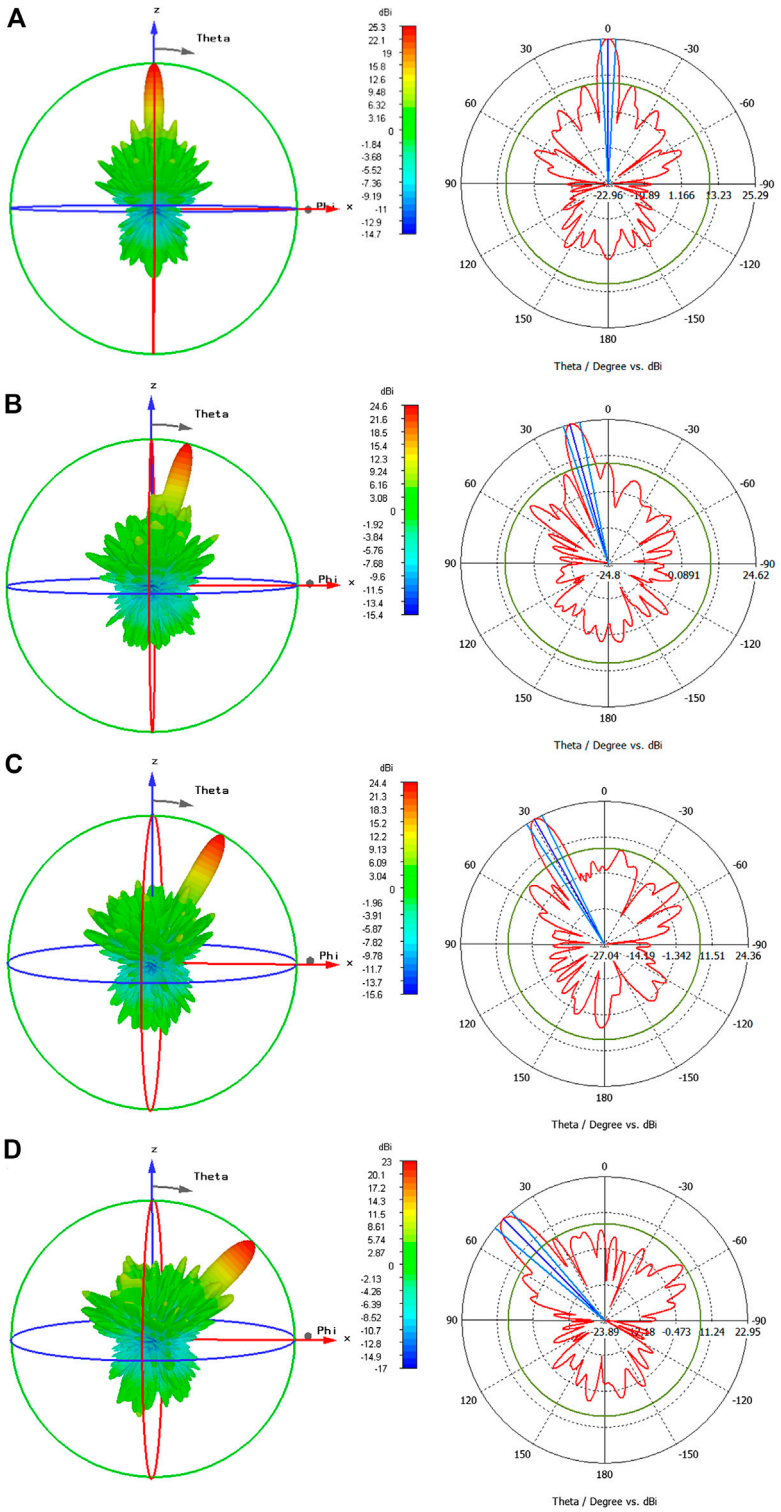

FIGURE 5 | Simulated 3-D and 2-D far-field radiation patterns for four beam directions **(A)** $\theta = 0^{\circ}$ **(B)** $\theta = 15^{\circ}$ **(C)** $\theta = 30^{\circ}$ **(D)** $\theta = 45^{\circ}$.

CONCLUSION

In summary, a high-efficiency transmissive programable metasurface with 1-bit phase modulation is presented for the construction of a cost-effective phased array. The expected performances with real-time dynamic scanning beams are investigated, and scanning pencil beams in four directions with low side-lobe levels are generated through dynamically programming the 1-bit code distributions on the metasurface, which verify the effectiveness of the presented transmissive programable metasurface design.

DATA AVAILABILITY STATEMENT

The original contributions presented in the study are included in the article, further inquiries can be directed to the corresponding author.

AUTHOR CONTRIBUTIONS

AC, ZC, KF, YY, and CH designed and performed the research as well as wrote the paper.

REFERENCES

1. Li A, Singh S, Sievenpiper D. Metasurfaces and their applications. *Nanophotonics* (2018) **7**:989–1011. doi:10.1515/nanoph-2017-0120
2. He Q, Sun S, Xiao S, Zhou L. High-effiiency metasurfaces: principles, realizations, and applications. *Adv Opt Mater* (2018) **6**:1800415. doi:10.1002/adom.201800415
3. Li Z, Premaratne M, Zhu W. Advanced encryption method realized by secret shared phase encoding scheme using a multiwavelength metasurface. *Nanophotonics* (2020) **9**:3687. doi:10.1515/nanoph-2020-0298
4. Li A, Li Y, Forati E, Kim S, Lee J, Long J, et al. Direct conversion of static voltage to a steerable RF radiation beam using an active metasurface. *IEEE Trans Antennas Propag* (2020) **68**:1680–8. doi:10.1109/TAP.2019.2934903
5. Bai X, Cao A, Kong F, Qian J, Xu S, Yan W, et al. Rotman lens-fed Fabry–Perot resonator antennas for generating converged multi-mode OAM beams. *IEEE Access* (2019) **7**:105768–75. doi:10.1109/ACCESS.2019.2932199
6. Raeker BO, Rudolph SM. Arbitrary transformation of antenna radiation using a cylindrical impedance metasurface. *Antennas Wirel Propag Lett* (2016) **15**:1101–4. doi:10.1109/LAWP.2015.2494739
7. Sun J, Chen K, Ding G, Guo W, Zhao J, Feng Y, et al. Achieving directive radiation and broadband microwave absorption by an anisotropic metasurface. *IEEE Access* (2019) **7**:93919–26. doi:10.1109/ACCESS.2019.2928839
8. Li A, Li Y, Long J, Forati E, Du Z, Sievenpiper D. Time-moduated nonreciprocal metasurface absorber for surface waves. *Opt Lett* (2020) **45**:1212–5. doi:10.1364/OL.382865
9. Li A, Kim S, Luo Y, Li Y, Long J, Sievenpiper DF. High-power transistor-based tunable and switchable metasurface absorber. *IEEE Trans Microw Theor Tech* (2017) **65**:2810–8. doi:10.1109/TMTT.2017.2681650
10. Akram MR, Ding G, Chen K, Feng Y, Zhu W. Ultra-thin single layer metasurfaces with ultra-wideband operation for both transmission and reflection. *Adv Mater* (2020) **32**:1907308. doi:10.1002/adma.201907308
11. Bai X, Kong F, Sun Y, Wang G, Qian J, Li X, et al. High-efficiency transmissive programmable metasurface for multimode OAM generation. *Adv Optical Mater* (2020) **8**:2000570. doi:10.1002/adom.202000570
12. Akram MR, Mehmood MQ, Bai X, Jin R, Premaratne M, Zhu W. High efficiency ultra-thin transmissive metasurfaces. *Adv Opt Mater* (2019) **7**:1801628. doi:10.1002/adom.201801628
13. Bai X. High-efficiency transmissive metasurface for dual-polarized dual-mode OAM generation. *Results Phys* (2020) **18**:103334. doi:10.1016/j.rinp.2020.103334
14. Zhuang Y, Wang G, Liang J, Zhang Q. Dual-band low-scattering metasurface based on combination of diffusion and absorption. *IEEE Antennas Wirel Propag Lett* (2017) **16**:2606–9. doi:10.1109/LAWP.2017.2735483
15. Saifullah Y, Waqas AB, Yang G-M, Zhang F, Xu F. 4-bit optimized coding metasurface for wideband RCS reduction. *IEEE Access* (2019) **7**:122378–86. doi:10.1109/ACCESS.2019. 2937849
16. Liu X, Gao J, Xu L, Cao X, Zhao Y, Li S. A coding diffuse metasurface for RCS reduction. *IEEE Antennas Wirel Propag Lett* (2017) **16**:724–7. doi:10.1109/LAWP. 2016.2601108
17. Yurduseven O, Marks DL, Gollub JN, Smith DR. Design and analysis of a reconfigurable holographic metasurface aperture for dynamic focusing in the Fresnel zone. *IEEE Access* (2017) **5**:15055–65. doi:10.1109/ACCESS.2017.2712659
18. Ramalingam S, Balanis CA, Birtcher CR, Shaman HN. Polarization-diverse holographic metasurfaces. *IEEE Antennas Wirel Propag Lett* (2019) **18**:264–8. doi:10.1109/LAWP.2018. 2888811
19. Amer AAG, Sapuan SZ, Nasimuddin N, Alphones A, Zinal NB. A comprehensive review of metasurface structures suitable for RF energy harvesting. *IEEE Access* (2020) **8**:76433–52. doi:10.1109/ACCESS.2020.2989516
20. Bai X. Polarization-insensitive reflective metasurfaces for highly efficient generation of OAM beams. *Front Physics* (2020) **8**:244. doi:10.3389/fphy.2020.00244
21. Akram Z, Li X, Qi Z, Aziz A, Yu L, Zhu H, et al. Broadband high-order OAM reflective metasurface with high mode purity using subwavelength element and circular aperture. *IEEE Access* (2019) **7**:71963–71. doi:10.1109/ACCESS.2019.2919779
22. Bai X, Kong F, Qian J, Song Y, He C, Liang X, et al. Polarization-insensitive metasurface lens for efficient generation of convergent OAM beams. *IEEE Antennas Wirel Propag Lett* (2019) **18**:2696–700. doi:10.1109/LAWP.2019.2949085
23. Akram MR, Bai X, Jin R, Vandenbosch GAE, Premaratne M, Zhu W. Photon spin Hall effect based ultra-thin transmissive metasurface for efficient generation of OAM waves. *IEEE Trans Antennas Propag* (2019) **67**:4650–8. doi:10.1109/TAP.2019.2905777
24. Akram MR, Mehmood MQ, Tauqeer T, Rana AS, Rukhlenko ID, Zhu W. Highly efficient generation of Bessel beams with polarization insensitive metasurfaces. *Optic Express* (2019) **27**:9467–80. doi:10.1364/OE.27.009467
25. Liu S, Xu H-X, Zhang HC, Cui TJ. Tunable ultrathin mantle cloak via varactor-diode-loaded metasurface. *Optic Express* (2014) **22**:13403–17. doi:10.1364/OE.22.013403
26. Della Giovampaola C, Engheta N. Digital metamaterials. *Nat Mater* (2014) **13**:1115–21. doi:10.1038/NMAT4082
27. Liu S, Cui TJ. Concepts, working principles and applications of coding and programmable metamaterials. *Adv Opt Mater* (2017) **5**:1700624. doi:10.1002/adom. 20170062410.1002/adom.201700624
28. Wan X, Qi MQ, Chen TY, Cui TJ. Field-programmable beam reconfiguring based on digitally controlled coding metasurface. *Sci Rep* (2016) **6**:20663. doi:10.1038/srep20663
29. Han J, Li L, Yi H, Shi Y. 1-bit digital orbital angular momentum vortex beam generator based on a coding reflective metasurface. *Opt Mater Express* (2018) **8**:3470–8. doi:10.1364/OME.8.003470
30. Zhang L, Chen XQ, Shao RW, Dai JY, Cheng Q, Castaldi G, et al. Breaking reciprocity with space-time-coding digital metasurfaces. *Adv Mater* (2019) **31**:1904069. doi:10.1002/adma. 201904069
31. Han J, Li L, Yi H, Xue W. Versatile orbital angular momentum vortex beam generator based on reconfigurable reflective metasurface. *Jpn J Appl Phys* (2018) **57**:120303. doi:10.7567/JJAP.57.120303
32. Clemente A, Dussopt L, Sauleau R, Potier P, Pouliguen P. Wideband 400-element electronically reconfigurable transmitarray in X band. *IEEE Trans Antenn Propag* (2013) **61**:5017–27. doi:10.1109/tap.2013.2271493
33. Wang M, Xu S, Yang F, Hu N, Xie W, Chen Z. A novel 1-bit reconfigurable transmitarray antenna using a C-shaped probe-fed patch element with

broadened bandwidth and enhanced efficiency. *IEEE Access* (2020) **8**: 120124–33. doi:10.1109/ACCESS.2020.3004435
34. Nguyen BD, Pichot C. Unit-cell loaded with PIN diodes for 1-bit linearly polarized reconfigurable transmitarrays. *IEEE Antennas Wirel Propag Lett* (2019) **18**:98–102. doi:10.1109/LAWP.2018.2881555
35. Wang Y, Xu S, Yang F, Li M. A novel 1-bit wide-angle beam scanning reconfigurable transmitarray antenna using an equivalent magnetic dipole element. *IEEE Trans Antennas Propag* (2020) **68**:5691–5. doi:10.1109/TAP.2020.2964954
36. MACOM. MA4FCP305 flip chip PIN diodes, (2018) Available from: http://cdn.macom.com/datasheets/MA4FCP305.pdf (Accessed March, 2018).

Conflict of Interest: The authors declare that the research was conducted in the absence of any commercial or financial relationships that could be construed as a potential conflict of interest.